Available online at www.sciencedirect.com
SCIENCE DIRECT®
Journal of Sound and Vibration 260 (2003) 537–547
JOURNAL OF SOUND AND VIBRATION
www.elsevier.com/locate/jsvi

Experiments on large-amplitude vibrations of a circular cylindrical panel

M. Amabili*, M. Pellegrini, M. Tommesani

Dipartimento di Ingegneria Industriale, Università di Parma, Parco Area delle Scienze 181/A, 43100 Parma, Italy

Received 2 January 2002; accepted 21 February 2002

Abstract

The vibration response of a thin circular cylindrical panel to harmonic excitation in the neighborhood of the first three natural frequencies has been measured for different force levels. The experimental boundary conditions approximate (i) on the curved edges: zero radial, axial and circumferential displacements; all rotations were allowed; (ii) on the straight edges: zero radial and axial displacements; all rotations and circumferential displacements were allowed. The different levels of excitation permitted reconstruction of the relatively strong, softening type non-linearity of the panel.

1. Introduction

Amabili and Païdoussis [1] recently compiled an extensive review of work on geometrically non-linearity (large-amplitude) vibrations of shells and curved panels. It was found that not many experimental investigations on large-amplitude vibrations of empty and fluid-filled circular cylindrical shells are available. In particular, it seems that experiments on non-linearity vibrations of circular cylindrical panels were reported only in the work of Nagai et al. [2], but the trend of non-linearity, which is obtained by performing tests with different levels of the excitation force, was not given. Also other experiments on non-linearity dynamics of curved panels are very scarce. Palazotto et al. [3] tested composite circular cylindrical panels subjected to impact, and Morino et al. [4] reported data of experiments on explosively loaded, clamped, circular cylindrical panels.

*Corresponding author. Tel.: 39-0521-905-896; fax: +39-0521-905-705.
E-mail address: marco@me.unipr.it (M. Amabili).
URL: http://me.unipr.it/mam/amabili/amabili.html.

0022-460X/03/$ - see front matter
PII: S0022-460X(02)00959-8

Many theoretical and numerical studies are available on geometrically non-linear vibration of circular cylindrical panels with different boundary conditions; see e.g., the review by Amabili and Païdoussis [1] and the papers of Leissa and Kadi [5], Hui [6], Fu and Chia [7] and Raouf [8].

The experimental response of panels as a function of the frequency of harmonic excitation and vibration amplitude, which was not available before the present study, is fundamental for validation of non-linearity shell theories and solution algorithms. For this reason, experiments on large-amplitude vibrations of a circular cylindrical panel with rectangular boundary were performed in the present study. The experimental boundary conditions approximate (i) on the curved edges: zero radial, axial and circumferential displacements; all rotations were allowed; (ii) on the straight edges: zero radial and axial displacements; all rotations and circumferential displacement were allowed.

2. Experimental set-up

Tests have been conducted on a circular cylindrical panel made of stainless steel. The dimensions and material properties of the panel are: length between supports $L = 522\,\text{mm}$, radius of curvature $R = 150\,\text{mm}$, thickness $h = 0.295\,\text{mm}$, angular width between supports 71° (curvilinear width length $b = 185\,\text{mm}$), Young's modulus $E = 1.95 \times 10^{11}\,\text{Pa}$, mass density $\rho = 7850\,\text{kg/m}^3$ and the Poisson ratio $v = 0.3$. The panel was inserted into a heavy rectangular frame made of several thick parts, see Fig. 1, having grooves designed to hold the panel. The frame was built with a mobile side, a screw and a load cell to give the desired axial load to the panel. Since the depth of the grooves was 0.5 mm, silicon was placed into the grooves to hold better the edges of the panel and then avoid radial displacements at the edges. The axial displacements at the straight edges and the circumferential displacements at the curved edges were prevented by friction between the panel and the grooves and by silicon. In fact, axially the panel had a small compression (the compressive load has been measured to be about 100 N and has absolutely negligible effects on natural frequencies and non-linearity response; in fact, the critical

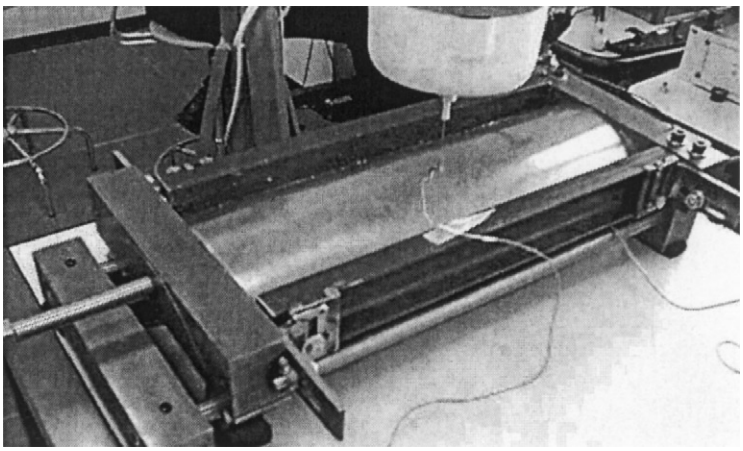

Fig. 1. Photograph of the experimental set-up.

load computed by using the approximate formula [9].

$$F_{cr} = \frac{Ebh}{6(1-\nu^2)}\left[\sqrt{12(1-\nu^2)(h/R)^2 + (\pi h/b)^4} + (\pi h/b)^2\right],$$

is 13960 N, which is very far from 100 N), which prevents axial displacement at the curved edges and increases the friction between grooves and panel's curved edges. The circumferential displacements on straight edges were allowed because the constraint given by silicon on this displacement was small.

The panel has been subjected to (i) burst-random excitation to identify the natural frequencies and perform a modal analysis by measuring the panel response on a grid of points, (ii) harmonic excitation, increasing or decreasing by very small steps the excitation frequency in the spectral neighbourhood of the lowest natural frequencies to characterize non-linearity responses in the presence of large-amplitude vibrations. The excitation has been provided by an electrodynamical exciter (shaker), model LDS V406 with power amplifier LDS PA100E, connected to the shell by a thin stinger glued in a position close to the centre of the panel; in particular 4 mm away axially and 2 mm away circumferentially. A piezoelectric force transducer, model B&K 8200, of mass 21 g, placed on the shaker and connected to the panel with a stinger, measured the force transmitted. The shell response has been measured by using a sub-miniature accelerometer, model Endevco 22, of mass 0.14 g. For all non-linearity tests, the accelerometer have been glued at the middle of the panel length at different angular positions corresponding to the antinode of the mode excited. The specific angular locations of the accelerometers are given in Table 1 for the different modes investigated. The time responses have been measured by using the Difa Scadas II front-end connected to a HP c3000 workstation and the software CADA-X of LMS for signal processing and data analysis; the same front-end has been used to generate the excitation signal. The CADA-X closed-loop control has been used to keep constant the value of the excitation force for any excitation frequency, during the measurement of the non-linearity response.

3. Natural frequencies and modes

The frequency response functions (FRFs) have been measured between 91 response points and one single excitation point. Both excitation force and measured responses have been in the radial direction. The response points have been located on a grid of seven equidistant arcs and 13

Table 1
Location $R\theta$ of the accelerometer in large-amplitude vibration tests; origin $\theta = 0$ at the centre of the panel; excitation at $R\,\theta = 2$ mm

Mode	Location
$n = 3$, $m = 1$	0 mm
$n = 2$, $m = 1$	−22 mm
$n = 4$, $m = 1$	−21 mm

positions on each arc. The experimental modal analysis has been performed by using the software CADA-X 3.5b of LMS and burst-random excitation with the following parameters: burst length 65%; frequency resolution 0.23 Hz; 10 averages; Hanning windows. The level of excitation was kept low in order to give small amplitude vibrations (approximating a linear system). The FRFs have been estimated by using the H_V technique. The modal parameters have been estimated by using the frequency domain, direct parameter identification technique. The analysis of the experimental data has been validated by using the modal assurance criterion and the modal phase collinearity.

The measured FRF in correspondence of the excitation (driven point) is shown in Fig. 2 with identification of natural modes. In the same figure, the FRF measured by using hammer excitation is also given in order to show the small added mass of the connection of the thin panel to the load cell and the shaker. The measured natural frequencies are presented and compared in Fig. 3 to numerical calculations with the FEM code ADINA 7.4; up to 1800 shell elements with 8 nodes have been used in the model (mesh refinement has been used to check convergence). Due to small geometric imperfections and sensors some modes are split in a couple of very similar modes with very close frequency. Each couple of modes is identified in Figs. 2 and 3 by the same indexes n and m, which are the number of circumferential and axial half-waves, respectively. In Fig. 4 four experimental and computed mode shapes are compared. Damping coefficients are given in the figure caption. The fundamental mode is ($n = 3$, $m = 1$). Theoretical and experimental results are in good agreement both in natural frequencies and mode shapes. In Table 2 a comparison of natural frequencies is given. This assures that the experimental boundary conditions approximate the constraints used in the FEM model, which are those summarized in Table 3.

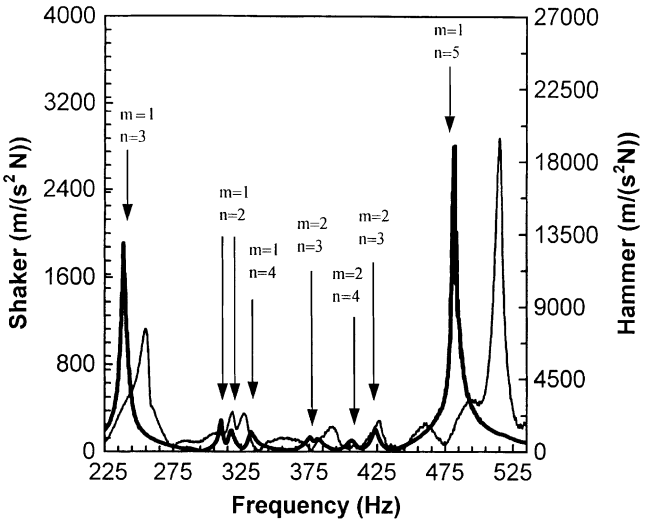

Fig. 2. Measured FRF of the driven point with identification of natural modes. —, excitation provided by shaker; —, hammer excitation.

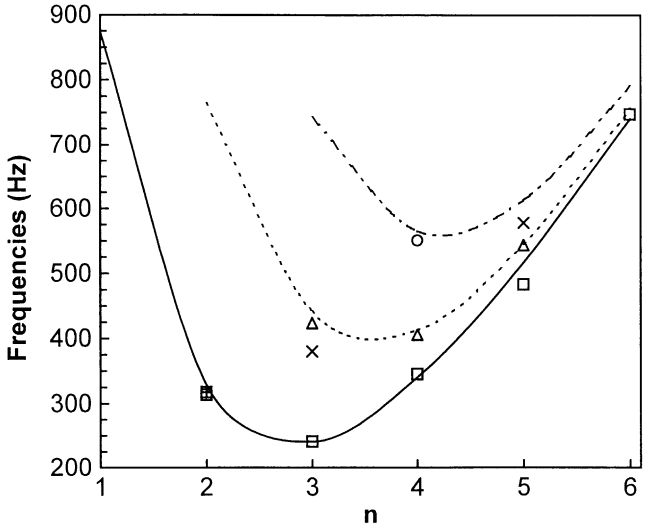

Fig. 3. Theoretical and experimental natural frequencies of the panel. Theoretical results: —, $m = 1$; – –, $m = 2$; –·–, $m = 3$. Experimental results: □, +, $m = 1$; △, ×, $m = 2$; ○, $m = 3$.

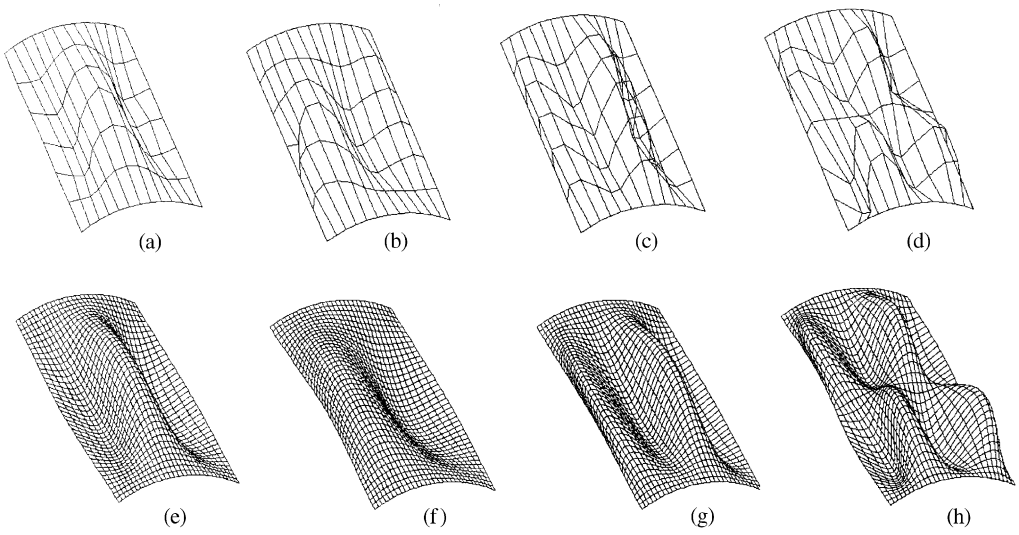

Fig. 4. Three-dimensional representation of measured and computed natural modes; all points at the intersection of two lines have been measured. (a) Measured fundamental mode ($n = 3$, $m = 1$), frequency 240.9 Hz, damping ratio 0.65%; (b) measured second mode ($n = 2$, $m = 1$), frequency 313.2 Hz, damping ratio 0.39%; (c) measured third mode ($n = 4$, $m = 1$), frequency 344.9 Hz, damping ratio 0.32%; (d) measured mode ($n = 4$, $m = 2$), frequency 405.7 Hz, damping ratio 0.85%; (e) computed fundamental mode ($n = 3$, $m = 1$), frequency 241.1 Hz; (f) computed second mode ($n = 2$, $m = 1$), frequency 328.6 Hz; (g) computed third mode ($n = 4$, $m = 1$), frequency 340.3 Hz; (h) computed mode ($n = 4$, $m = 2$), frequency 412.9 Hz.

Table 2
Natural frequencies obtained by experiments, compared to FEM results

m	n	Experimental frequency (Hz)	FEM frequency (Hz)
1	2	313.2	328.6
1	2	317.1	328.6
1	3	240.9	241.1
1	4	344.9	340.3
1	5	482.6	516.7
1	6	747.7	741.0
2	3	423.4	441.6
2	3	380.4	441.6
2	4	405.7	412.9
2	5	577.7	545.4
2	5	543.7	545.4
3	4	551.0	564.9

Table 3
Boundary conditions used in FEM model (approximation of experimental constraints)

	Axial displ.	Radial displ.	Circumferential displ.	Rotations
Straight edges	Constrained	Constrained	Free	Free
Curved edges	Constrained	Constrained	Constrained	Free

4. Non-linearity results

Fig. 5 shows the measured accelerations around the fundamental frequency ($n = 3$, $m = 1$; natural frequency 240.9 Hz) versus the excitation frequency for five different force levels: 0.01, 0.1, 0.25, 0.5, and 0.7 N. The level of 0.01 N gives a very good evaluation of the natural (linear) frequency. The closed-loop control used in the experiments keeps the magnitude of the harmonic excitation force constant after filtering the signal from the load cell in order to use only the harmonic component with the given excitation frequency. The measured accelerations reported in Fig. 5 have been filtered in order to eliminate any frequency except the excitation frequency. Experiments have been performed with both increasing and decreasing the excitation frequency; the frequency step used in this case is 0.025 Hz, 16 periods have been measured with 64 points per period and 50 periods have been waited before data acquisition every time that the frequency is changed. The hysteresis between the two curves (up = increasing frequency; down = decreasing frequency) is clearly visible. Sudden increments (jumps) of the vibration amplitude are observed when increasing and decreasing the excitation frequency; these are characteristic of a softening type non-linearity. The measured accelerations have been converted to displacements, dividing by the excitation circular frequency squared, and have been plotted in Fig. 6. The graph has been made non-dimensional by dividing the displacements by the panel thickness h and the excitation frequencies by dividing by the natural circular frequency $\omega_{m,n} = 240.92 \times 2\pi$. When the vibration

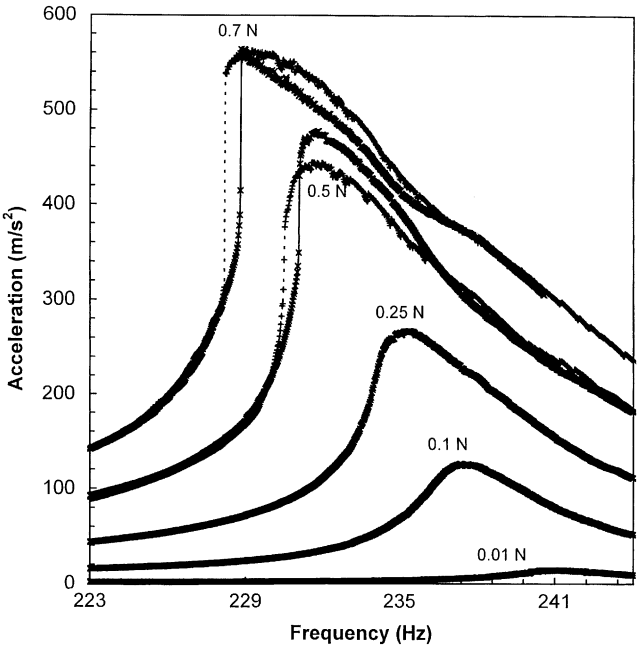

Fig. 5. Experimentally measured acceleration (peak) versus excitation frequency with different harmonic forces; fundamental mode ($n = 3$, $m = 1$). —×—, increasing the excitation frequency; – –+– –, decreasing the excitation frequency.

amplitude is equal to 0.9 times the shell thickness, the peak of the response appears for a frequency lower of about 5% with respect to the linear one (i.e., the one measured with force 0.01 N). The phase relationships between the acceleration (measured positive outwards) and the force input (measured positive inwards) are given in Fig. 7.

The experimental force input and acceleration for the fundamental mode ($n = 3$, $m = 1$) of the panel are shown in Fig. 8 versus time for excitation of magnitude 0.5 N and frequency 225.1 Hz measured by increasing the excitation frequency. In these conditions, the shell response is the one obtained before the big jump (sudden decrement of the response amplitude) on the left of peak in Fig. 6 for a force of 0.5 N. The input force simulates accurately a sinusoidal function of time and the measured accelerations are relatively small. The experimental force input and acceleration for the same level of excitation but a frequency of 233.15 Hz (measured by increasing the excitation frequency) are shown in Fig. 9. In these conditions, the shell response is the one at the peak in Fig. 6 for force of 0.5 N. The input force is no more a pure sinusoidal function of time and the measured acceleration is quite large and distorted. For acceleration very close to the peak, the corresponding input force has been found to be similarly distorted for forces of 0.5 N or larger. This distortion causes some differences (where these are not due to softening type non-linearity) between the two curves measured increasing and decreasing the excitation frequency around the peak of the response.

Measured responses of the second ($n = 2$, $m = 1$) and third ($n = 4$, $m = 1$) mode of the panel for different force levels are given in Figs. 10 and 11, respectively. Remarkable softening type

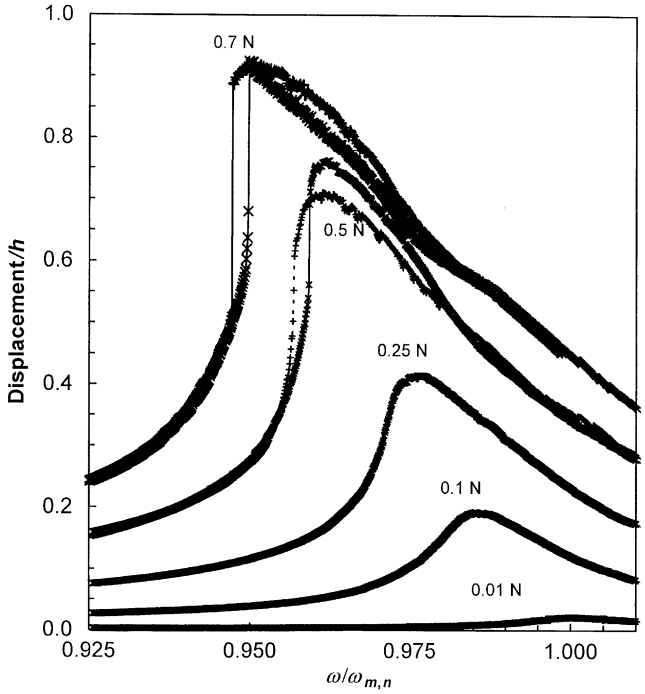

Fig. 6. Non-dimensional oscillatory displacement (peak) versus non-dimensional excitation frequency with different harmonic forces; fundamental mode ($n = 3$, $m = 1$). — × —, increasing the excitation frequency; – –+– –, decreasing the excitation frequency.

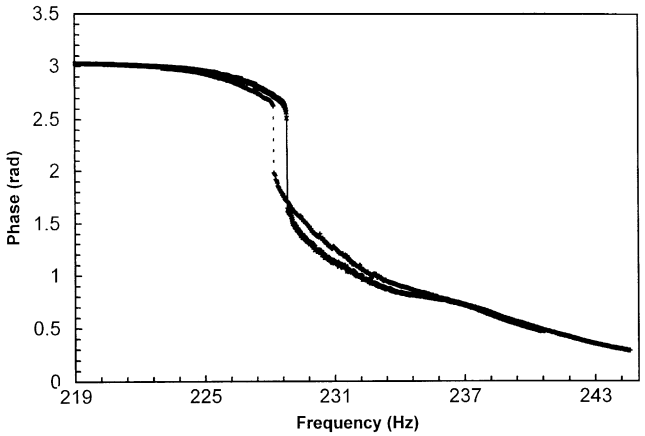

Fig. 7. Experimentally measured response phase–frequency curves for the fundamental mode; force 0.7 N. — × —, increasing the excitation frequency; – –+– –, decreasing the excitation frequency.

non-linearity is clearly visible also for these modes. In Fig. 10 a second rounded peak can be observed for the response to excitation of 3 N; this is exactly the same mode ($n = 2$, $m = 1$) with a slightly different frequency due to geometric imperfections, connection to the shaker and accelerometer.

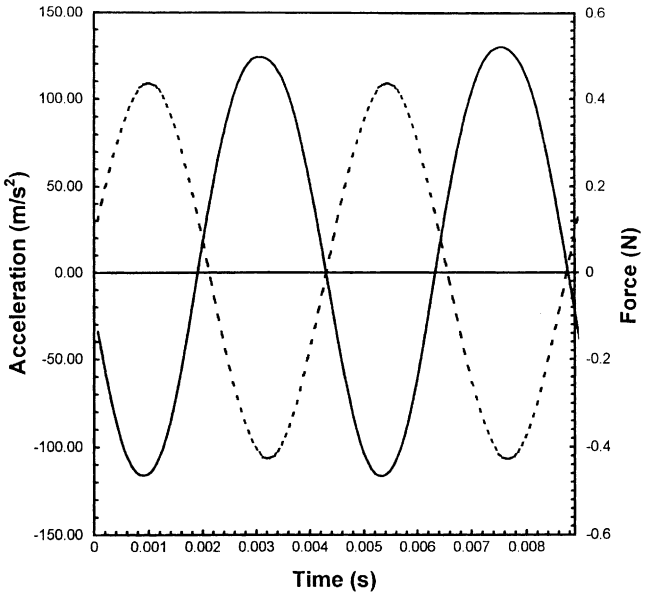

Fig. 8. Measured force and acceleration (peak) versus time for the fundamental mode ($n = 3$, $m = 1$); force 0.5 N, frequency 225.1 Hz increasing frequency. ——, force; – –, acceleration.

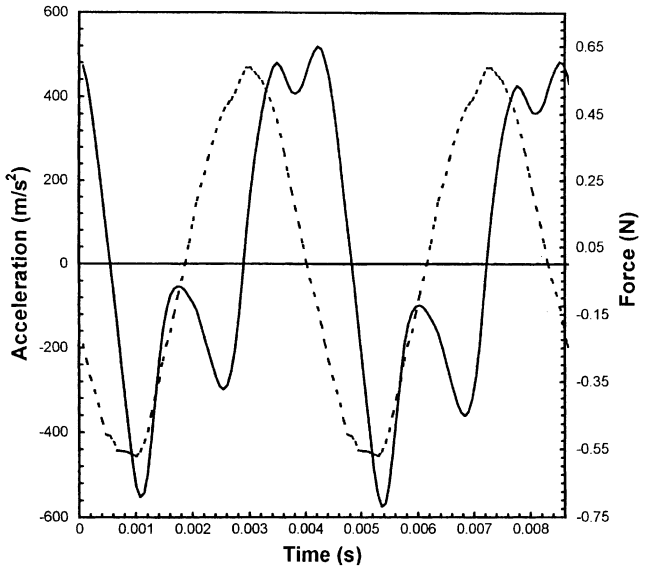

Fig. 9. Measured force and acceleration (peak) versus time for the fundamental mode ($n = 3$, $m = 1$); force 0.5 N, frequency 233.15 Hz increasing frequency. ——, force; – –, acceleration.

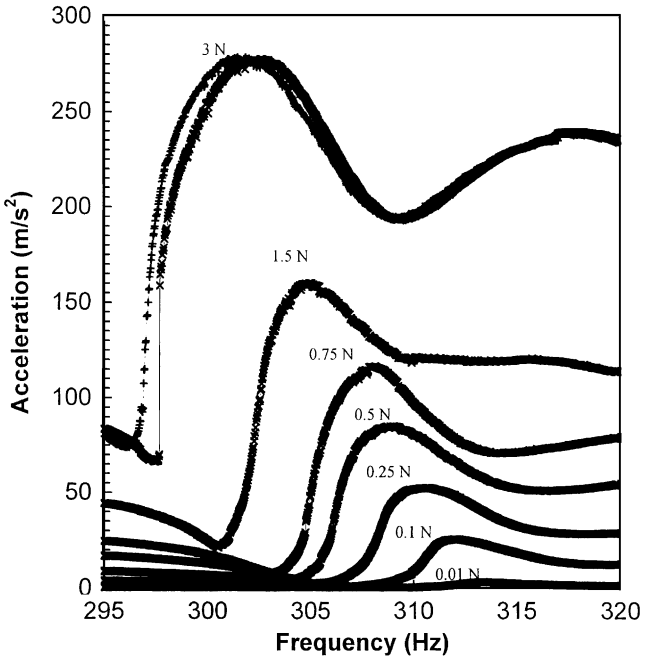

Fig. 10. Experimentally measured acceleration versus excitation frequency with different harmonic forces; second mode ($n = 2$, $m = 1$). —×—, increasing the excitation frequency; – –+– –, decreasing the excitation frequency.

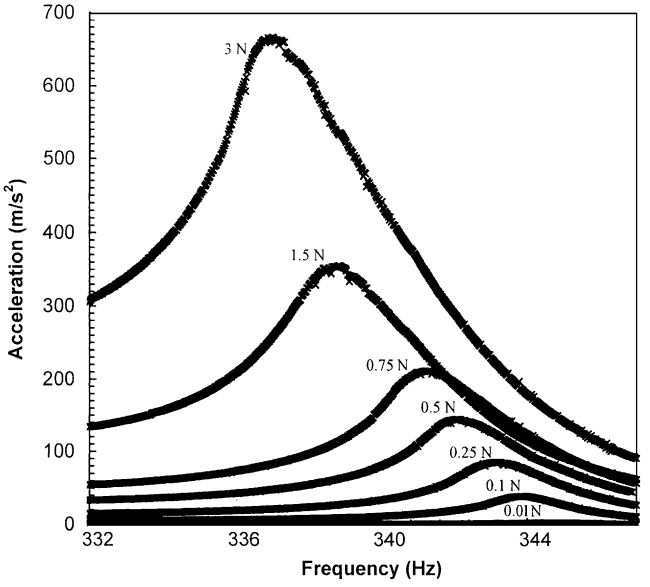

Fig. 11. Experimentally measured acceleration versus excitation frequency with different harmonic forces; third mode ($n = 4$, $m = 1$). —×—, increasing the excitation frequency; – –+– –, decreasing the excitation frequency.

5. Conclusions

Experiments show that the curved panel tested presents a relatively strong geometric non-linearity of softening type. In particular, for the fundamental mode the resonance is reached for frequency 5% lower than the natural (linear) frequency when the vibration amplitude is equal to 0.9 times the shell thickness. This is particularly interesting when these results are compared to the non-linearity of the fundamental mode of complete (closed around the circumference), simply supported, circular cylindrical shells of similar length and radius, which present much weaker nonlinearity [1].

Acknowledgements

This work was partially supported by the COFIN 2000 grant of the Italian Ministry for University and Research (MURST).

References

[1] M. Amabili, M.P. Païdoussis, Review of studies on geometrically nonlinear vibrations and dynamics of circular cylindrical shells and panels, with and without fluid-structure interaction, Applied Mechanics Reviews, in press.
[2] K. Nagai, T. Yamaguchi, T. Murata, Chaotic oscillations of a cylindrical shell-panel with concentrated mass under gravity and cyclic load, Proceedings of the Third International Symposium on Vibration of Continuous Systems, Grand Teton National Park, WY, July 23–27, 2001, pp. 49–51.
[3] A.N. Palazotto, R. Perry, R. Sandhu, Impact response of graphite/epoxy cylindrical panels, American Institute of Aeronautics and Astronautics Journal 30 (1992) 1827–1832.
[4] L. Morino, J.W. Leech, E.A. Witmer, An improved numerical calculation technique for large elastic–plastic transient deformations of thin shells. Part 2—evaluation and applications, American Society of Mechanical Enginners Journal of Applied Mechanics 38 (1971) 429–436.
[5] A.W. Leissa, A.S. Kadi, Curvature effects on shallow shell vibrations, Journal of Sound and Vibration 16 (1971) 173–187.
[6] D. Hui, Influence of geometric imperfections and in-plane constraints on nonlinear vibrations of simply supported cylindrical panels, American Society of Mechanical Enginners Journal of Applied Mechanics 51 (1984) 383–390.
[7] Y.M. Fu, C.Y. Chia, Multi-mode non-linearity vibration and postbuckling of anti-symmetric imperfect angle-ply cylindrical thick panels, International Journal of Non-Linearity Mechanics 24 (1989) 365–381.
[8] R.A. Raouf, A qualitative analysis of the nonlinear dynamic characteristics of curved orthotropic panels, Composites Engineering 3 (1993) 1101–1110.
[9] W.C. Young, Roark's Formulas For Stress and Strain, 6th Edition, McGraw-Hill, New York, 1989.